Superior mechanical properties of Nb_2AsC to those of other layered ternary carbides: a first-principles study

2006 J. Phys.: Condens. Matter 18 L527

(http://iopscience.iop.org/0953-8984/18/41/L04)

INSTITUTE OF PHYSICS PUBLISHING JOURNAL OF PHYSICS: CONDENSED MATTER

J. Phys.: Condens. Matter **18** (2006) L527–L533 doi:10.1088/0953-8984/18/41/L04

LETTER TO THE EDITOR

Superior mechanical properties of Nb_2AsC to those of other layered ternary carbides: a first-principles study

Ting Liao[1,2], **Jingyang Wang**[1,3] **and Yanchun Zhou**[1]

[1] High-performance Ceramic Division, Shenyang National Laboratory for Materials Science, Institute of Metal Research, Chinese Academy of Sciences, Shenyang 110016, People's Republic of China
[2] Graduate School of Chinese Academy of Sciences, Beijing 100039, People's Republic of China
[3] International Centre for Materials Physics, Institute of Metal Research, Chinese Academy of Sciences, Shenyang 110016, People's Republic of China

Received 2 August 2006
Published 29 September 2006
Online at stacks.iop.org/JPhysCM/18/L527

Abstract

Nb_2AsC showed superior mechanical properties to those of other layered ternary carbides (Kumar *et al* 2005 *Appl. Phys. Lett.* **86** 111904). In the present density functional calculation, the underlying mechanism is interpreted by astonishing bonding features of Nb_2AsC. The Nb d–As ($p_x + p_y$) and Nb d–As p_z bonding states locate in the same energy range as those of Nb d–C p bonding, which indicates that the Nb–As bond has similar bonding strength as the Nb–C bond does; and thereafter, Nb_2AsC has improved mechanical properties compared to the others. The present reported bonding features are interestingly different from those experienced by T_2AlC (T = Ti, V, Cr, and Nb), wherein the weak T–Al coupling was separated from T–C bonding states in the higher energy level by a pseudogap. This work proposes an effective method to strengthen the relative weaker T–A (A is the A-group element) bonding in layered ternary carbides.

(Some figures in this article are in colour only in the electronic version)

Layered ternary carbides with the common formula $T_{n+1}AX_n$ (where T is a transition metal, A is an A-group element, and X is C) are promising damage-tolerant ceramics with interesting properties [1]. They exhibit merits of both metals and high-performance ceramics such as good thermal and electrical conductivity, excellent thermal shock resistance and high-temperature oxidation resistance, and microscale ductility at room temperature. Recently, optimization of mechanical properties was the most concentrated subject for TAX carbides by properly tuning the valence electron concentration (VEC) in material [2–4]. Barsoum *et al* succeeded in strengthening Ti_2AlC by synthesizing the $Ti_2AlC_{0.5}N_{0.5}$ solid solution [2]. Later, theoretical calculations by Wang *et al* [3] and Sun *et al* [4] suggested an alternative way by tailoring the transition-metal atom in T_2AlC (T = Ti, V, Cr and Nb). Increased bulk modulus and elastic

coefficient c_{44} were achieved therein. The mechanism was attributed to strengthening of T d–Al p bonding when the VEC increased [3].

The crystal structure of layered ternary carbides can be described as TC slabs in an NaCl-type structure being interleaved and mirrored by close-packed A-element atomic planes. The mechanical properties of TAX carbides are dominated by the weak coupling between transition-metal carbide/nitride slabs and the interleaved A-element atomic planes [5]. It is necessary to find an effective method to strengthen the T–A bonding in TAX material. Recently, a room-temperature synchrotron x-ray diffraction experiment was conducted on Nb_2AsC in the pressure range up to 41 GPa [6]. It was reported that Nb_2AsC yielded the highest bulk modulus (224 GPa) in the TAX carbides measured to date. In addition, the compressibility along the basal plane is higher than along the c-direction, which is different to other TAX carbides such as Ti_3SiC_2 [7] and Ti_2AlC [8]. The underlying mechanism of superior mechanical properties of Nb_2AsC should be investigated, and the results of continued research in this area may play a key role in better understanding the mechanical properties of ternary TAX carbides. In the present density functional calculations, the elastic stiffness and ideal shear strength were calculated and interpreted by interesting bonding characteristics. For comparison, electronic structure analysis of Nb_2AlC was also performed. Specially, we suggest that mechanical properties of TAX carbides could be more effectively enhanced by tailoring the VEC of the A-element atoms.

The density functional calculations were performed using the CASTEP total energy code [9]; the Vanderbilt-type ultrasoft pseudopotential [10] and generalized gradient approximation (GGA-PW91) [11] were employed. The plane-wave basis set cutoff was set to 450 eV for all calculations. The special points sampling integration over the Brillouin zone was employed by using the Monkhorst–Pack method with a $10 \times 10 \times 2$ special k-point mesh [12]. The Broyden–Fletcher–Goldfarb–Shanno (BFGS) minimization scheme [13] was used in geometry optimization. Lattice parameters, including lattice constants and internal atomic coordinates, were modified independently to minimize the total energy and interatomic forces. The tolerances for geometry optimization are: difference on total energy within 5×10^{-6} eV/atom, maximum ionic Hellmann–Feynman force within 0.01 eV $Å^{-1}$, maximum ionic displacement within 5×10^{-4} Å, and maximum stress within 0.02 GPa.

To study interatomic bonding characteristics, the projected densities of states (PDOSs) were obtained within the full-potential linearized augmented plane-wave (FPLAPW) + local orbitals (lo) method implemented in the Wien2K code [14]. Separation radii between valence states and core states were 2.21, 2.50, and 1.96 au for the Nb, As, and C atoms, respectively, in Nb_2AsC; but were 2.17, 2.50, and 1.92 au for the Nb, Al, and C atoms, respectively, in Nb_2AlC. A $10 \times 10 \times 2$ special k-point mesh was used. The total energy was converged within 6.8×10^{-6} eV. The spheres separate the space between core states treated as atomic orbitals and valence states treated as plane waves in the interstitial space.

The elastic stiffness determines the response of a material to an externally applied strain or stress and provides information about the bonding characteristics and structural stability. The bulk modulus measures the resistance of a material to a volume change, and the shear modulus and shear strength determine how readily a dislocation is generated and is able to move throughout a solid in response to a shear strain or stress. Furthermore, shear deformation resistance is correlated to the hardness of a material and may serve as a suitable hardness predictor [15–17]. Therefore, mechanical parameters, including bulk modulus B, shear modulus c_{44}, and ideal shear strength σ, were investigated in the current work.

Theoretical elastic coefficients were determined by applying a set of given homogeneous deformations with a finite value and calculating the produced stress with respect to optimizing the internal atomic coordinates [3]. The criteria for convergences of geometry optimization

Table 1. Computed bulk modulus B (in GPa), elastic constant c_{44} (in GPa) and ideal shear strength τ (in GPa) of Ti_2AlC, Nb_2AlC, Cr_2AlC and Nb_2AsC.

Compound	B	c_{44}	c_{44}/B	τ
Ti_2AlC	137	111	0.810	11
Nb_2AlC	183	150	0.820	14
Cr_2AlC	193	147	0.762	11
Nb_2AsC	219	182	0.831	19

were set as: differences in the total energy within 1×10^{-6} eV/atom, ionic Hellmann–Feynman forces within 0.002 eV $Å^{-1}$, and the maximum ionic displacement within 1×10^{-4} Å.

In order to obtain the theoretical stress–strain relations, we applied a series of incremental strains to the crystal up to strains far beyond the linearity. At each step, the lattice parameters and internal atomic freedoms were simultaneously relaxed until all components of the Hellmann–Feynman stress tensor orthogonal to the applied strain converged within 0.2 GPa. The ideal shear strength was calculated as the first maximum shear stress in the theoretical stress–strain curve [17]. In the current investigation, the lattices were sheared along the $[1\bar{2}10](0001)$ deformation path. For comparison, the elastic stiffness and ideal shear stress–shear strain relationships were calculated for the Nb_2AsC, Ti_2AlC, Cr_2AlC and Nb_2AlC compounds. The present authors have investigated the theoretical stress–strain relationships for ternary compounds Ti_2AlC and Ti_2AlN, and binary counterparts TiC and TiN [18]. In addition, the obtained stress–strain relationships of TiC and TiN agreed well with those reported by Jhi and collaborators [19]. The present calculation is reliable for calculating the theoretical stress–strain relationships of layered ternary compounds and their binary counterparts.

Knowledge of elastic coefficients enables us to evaluate the ratio between linear compressibility coefficients in the directions along the basal plane and the c-direction using [20]

$$k_c/k_a = (c_{11} + c_{12} - 2c_{13})/(c_{33} - c_{13}) \tag{1}$$

where c_{ij} is second-order elastic coefficient. The values of k_c/k_a for Cr_2AlC and Nb_2AsC are 0.878 and 0.673, respectively, while the ratio is 1.139 for Ti_2AlC and 1.140 for Nb_2AlC. For Cr_2AlC and Nb_2AsC, the stiffness along the c-direction is higher than that along the basal plane. In contrast, Ti_2AlC and Nb_2AlC experience the reverse tendency, for which the c-direction is softer. The calculated compressibility agrees well with experimental results [6]. The underlying reason for the diverse compressibility tendency could be addressed to different coupling strengths between the transition-metal carbide slabs and A-element atomic planes. In Cr_2AlC and Nb_2AsC, the T–A bonding strengths are suggested as being enhanced over that in Ti_2AlC and Nb_2AlC. For compounds with hexagonal symmetry, the elastic coefficient c_{44} determines the elastic resistance against an applied $[1\bar{2}10](0001)$ shear strain. It has been reported that higher elastic coefficient c_{44} and, thus, improved mechanical properties (i.e., hardness) can be achieved by tuning the VEC of ternary T_2AlC (T = Ti, V, and Cr) carbides [3, 21]. The computed elastic coefficient c_{44} of Nb_2AsC is listed in table 1, together with those of Ti_2AlC, Nb_2AlC and Cr_2AlC for comparison. We note that Nb_2AsC has the highest c_{44} in these ternary compounds. This result suggests that Nb_2AsC may show improved mechanical properties dominated by the shear modulus c_{44}.

Ideal shear strength is the maximum shear stress that chemical bonding can sustain under shear deformation and is of particular importance for understanding the structural stability of a solid. Theoretically, we have shown that Ti_2AlC and Ti_2AlN experience small ideal shear strengths, which leads to damage tolerance and low hardness [18]. Therein, the authors

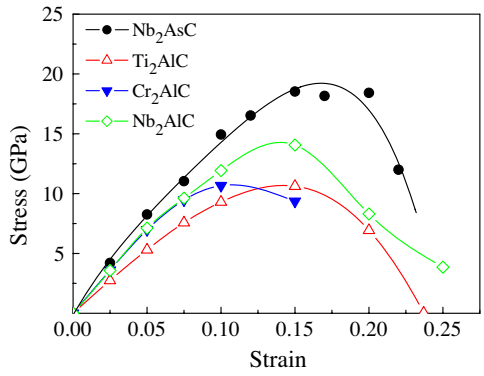

Figure 1. Theoretical stress–strain curves of Ti_2AlC, Nb_2AlC, Cr_2AlC and Nb_2AsC under applied $[1\bar{2}10](0001)$ shear strains.

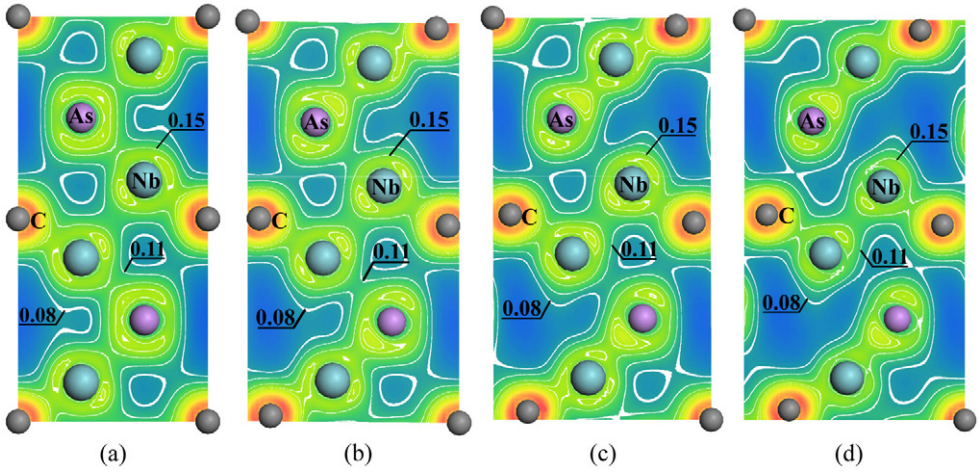

Figure 2. Valence electron density of a slice of the $(11\bar{2}0)$ plane in the Nb_2AsC unit cell under shear deformations of (a) $\varepsilon = 0$, (b) $\varepsilon = 0.1$, (c) $\varepsilon = 0.15$ and (d) $\varepsilon = 0.2$.

proposed that the ideal shear strengths of ternary compounds are much smaller than those of the binary counterparts, like TiC and TiN. Exploring enhanced ideal shear strength is expected to be important in predicting optimized mechanical properties of TAX carbides. In figure 1, we present the first-principles stress–strain curves of Ti_2AlC, Nb_2AlC, Cr_2AlC and Nb_2AsC under $[1\bar{2}10](0001)$ shear strains. As shown in figure 1, the stress of Nb_2AsC exhibits larger value than other carbides throughout the studied shear strains. The obtained ideal shear strength of Nb_2AsC is about 1.7, 1.4, and 1.7 times larger than that of Ti_2AlC, Nb_2AlC, and Cr_2AlC, respectively.

Figure 2 shows slices of valence electron density distribution in the $(11\bar{2}0)$ atomic plane of Nb_2AsC under $[1\bar{2}10](0001)$ shear strains. When Nb_2AsC is shear deformed, As atoms slip smoothly along the basal plane, and only half of the Nb–As bonds stretch and soften gradually according to the applied strain mode. In contrast, the strong Nb–C covalent bonds remain stable. The shear deformation proceeds smoothly by bond-softening rather than by an abrupt bond-breaking of the Nb–As bond. At a shear strain of 0.2, the stretched Nb–As bond reaches

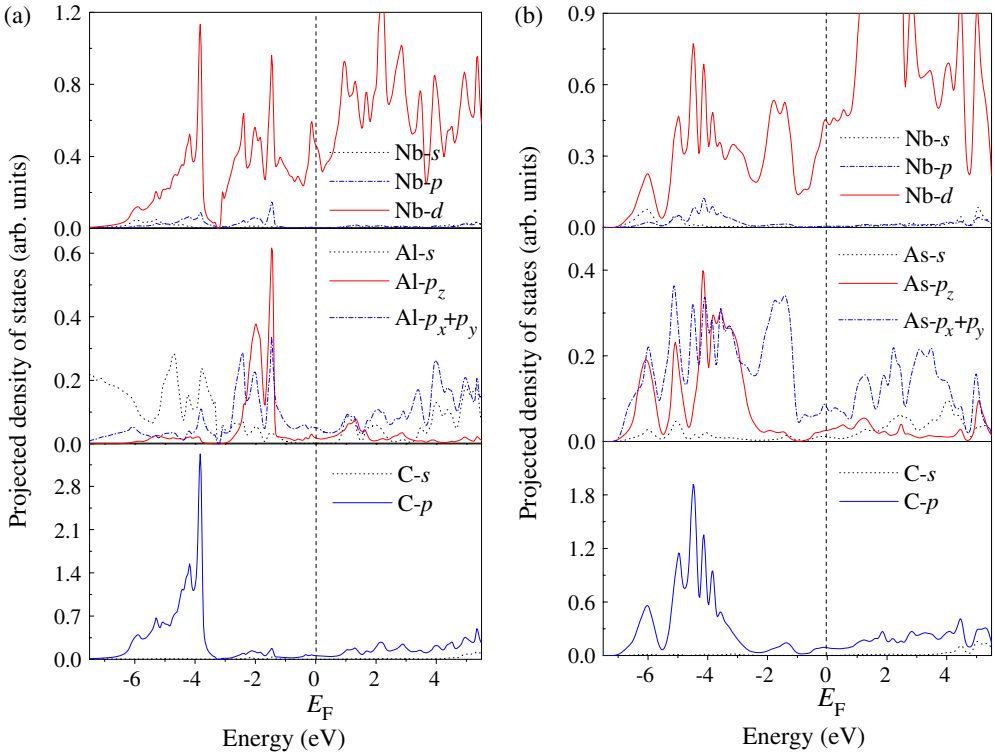

Figure 3. Projected electronic density of states of (a) Nb_2AlC and (b) Nb_2AsC.

its limit of stability and breaks eventually. This leads to the gradual stress relaxation at large strains.

As summarized in table 1, Nb_2AsC yields the highest bulk modulus B, shear modulus c_{44}, and ideal shear strength compared to Ti_2AlC, Nb_2AlC, and Cr_2AlC. Therefore, Nb_2AsC is expected to have significantly strengthened mechanical properties. It should be noted that Cr_2AlC and Nb_2AsC have the same average VEC in the unit cell. However, the theoretical mechanical parameters of Nb_2AsC are obviously higher than those of Cr_2AlC. Therefore, tailoring the A-element atoms may be more effective than tuning the VEC of transition-metal atoms to strengthen the TAX carbides. To better understand the origin of the superior mechanical properties of Nb_2AsC, interatomic bonding is characterized and compared with that of Nb_2AlC, a ternary carbide that differs from Nb_2AsC only in element A.

The projected electronic density of states (PDOS) of Nb_2AsC is illustrated in figure 3, together with those of Nb_2AlC. In figure 3(a), a pseudogap separates the strong covalent Nb–C bonding states from those of Nb–Al bonding orbitals. This bonding feature is mostly observed in Ti_2AlC, V_2AlC, and Cr_2AlC [3, 4]. However, as seen in figure 3(b), the bonding states in Nb_2AsC exhibit different features: the strong Nb d–C p bonding states approximately locate between -7.0 and -3.0 eV below the Fermi level; and in addition, the Nb d–As p_z and Nb d–As $p_x + p_y$ bonding states, ranging from -7.0 to -2.0 eV, locate approximately in the same energy level as that of the Nb–C bond; at the same time, relatively weaker Nb d–As ($p_x + p_y$) bonding states locate in higher energy level, extending from -2.0 to -1.0 eV. The Nb d–Nb d metallic bonding dominates states near the Fermi level. Of the most interest, the bonding strengths of Nb–C and Nb–As bonds are expected to have the same scale, suggested by the

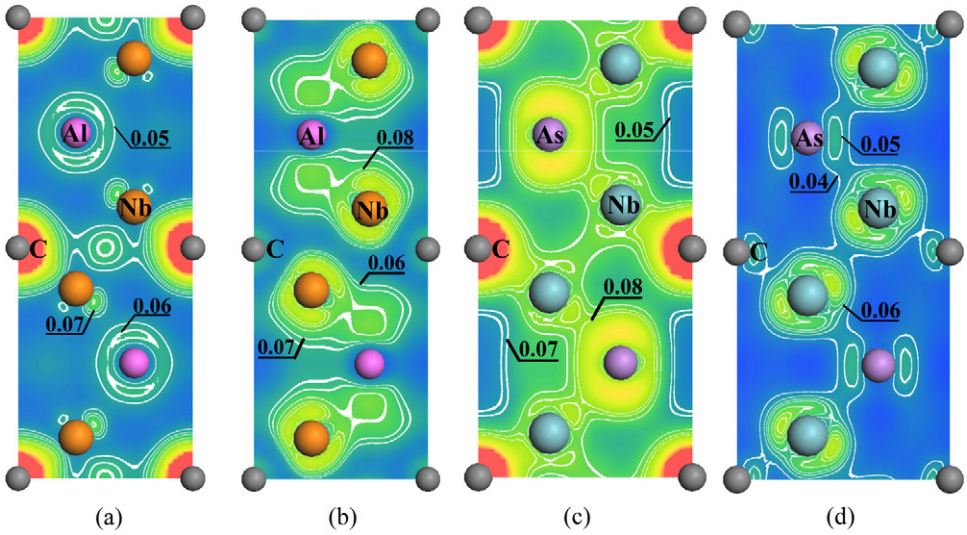

Figure 4. Valence electron density from different energy ranges of the DOS for Nb_2AlC and Nb_2AsC. The plots are in the $(11\bar{2}0)$ plane and the units are electron $Å^{-3}$. (a) Covers energies between −7.0 and −3.0 eV of Nb_2AlC, while (b) includes energies from −3.0 eV to the Fermi level. (c) and (d) are similar to (a) and (b) except for Nb_2AsC.

fact of their extending in the same energy level. This shows that the bonding characteristics of Nb_2AsC differ from those of Ti_2AlC, V_2AlC, Nb_2AlC and Cr_2AlC significantly. In those Al-containing ternary carbides, the bonding states associated to T–C and T–Al bonds extend in different energy levels and are separated by a noticeable pseudogap [3, 4]. Therein, the T–Al bond was definitely weaker than the T–C bond in T_2AlC (T = Ti, V, Cr, and Nb).

Since the bonding characters at different energy ranges appear to be responsible for the mechanical features of the studied compounds, it is of interest to examine the charge density decomposed into different covalent bonding peaks in the DOS figures, as shown in figure 4. The plots use electron $Å^{-3}$ as the unit of charge density. In figure 4(a), the charge density comes from states in the energy range between −7.0 and −3.0 eV for Nb_2AlC. It shows clear evidence of predominant p-like orbitals on the C sites, and t_{2g}-like orbitals on the Nb sites. Figure 4(b) illustrates the charge density originated from states in a higher energy level extending from −3.0 eV to the Fermi level for Nb_2AlC. It indicates that the charge density of Al atoms has p_z symmetry, as well as the $(e_g + t_{2g})$-like orbitals on the Nb sites. From figures 4(a) and (b), we found that the covalent bonding in Nb_2AlC is basically similar to that in Ti_2AlC, V_2AlC and Cr_2AlC. Figure 4(c) shows the charge density corresponding to states in Nb_2AsC extending in the same energy level as in figure 4(a). It is interesting to observe that charge density originated from Nb–As bonding is presented, besides those corresponding to strong Nb–C covalent bonding. The charge density in figure 4(d) derives from the states in energy level from −3.0 eV to the Fermi level of Nb_2AsC. It corresponds to the double peaks in the upper energy level in figure 3(b). In contrast to the bonding features in Nb_2AlC, wherein Nb–Al bonding has d–p_z bonding characteristics, the Nb–As bonding in Nb_2AsC exhibits obvious d–$p_x + p_y$ bonding characteristics.

Based on the bonding features of Nb_2AsC, its superior mechanical properties could be best understood in effectively enhanced Nb–As pd covalent bonding strength. Sufficient numbers of valence electrons provided by the As atoms cause the appearance of Nb d–As $(p_x + p_y)$

bonding, and thereafter, the Nb d–As p bonding states shift downward to the same energy level as those of the Nb–C bond. The stronger the T–A covalent bonding in Nb_2AsC, the higher resistance to applied strain is achieved. We have previously investigated mechanical properties of M_2AlC (M = Ti, V, Cr, and Nb) by changing the VEC in compounds [3]. It was found that the M d–Al p_z bonding strengthened when VEC increased. However, after the shear-deformation resistive M d–Al p_z bonding states were completely occupied, filling metallic d–d bonding states on the M site occurred. In terms of mechanical parameters, shear moduli reach maximum values and drop slightly thereafter. Compared to the results in the above-mentioned references, tailoring the VEC of A-element atoms, rather than the T atoms in layered TAX carbides, may be more effective in optimizing the mechanical properties.

In summary, interesting bonding characteristics and superior mechanical properties of Nb_2AsC are reported in the present letter. We found that Nb–As bonding states locate approximately in the same energy level as those of Nb–C bonding. This bonding characteristic is different from those of Al-containing ternary carbides, Ti_2AlC, Nb_2AlC, and Cr_2AlC, wherein the T–Al and T–C (T = Ti, Nb and Cr) bonds extend in two subgroups and are separated by a pseudogap. The results suggest that Nb–As and Nb–C bonds have similar bonding strength, and thereafter the bulk modulus, shear modulus c_{44} and ideal shear strength of Nb_2AsC are significantly enhanced. Finally, the present letter predicts underlying mechanisms toward strengthening ternary TAX carbides by tailoring the VEC of A-element atoms.

This work was supported by the National Outstanding Young Scientist Foundation for Y C Zhou under Grant No. 59925208, and the Natural Sciences Foundation of China under Grant Nos 50232040, 90403027 and 50302011.

References

[1] Barsoum M W 2000 *Prog. Solid State Chem.* **28** 201
[2] Barsoum M W, Ali M and El-Raghy T 2000 *Metall. Mater. Trans.* A **31** 1857
[3] Wang J Y and Zhou Y C 2004 *Phys. Rev.* B **69** 214111
[4] Sun Z M, Ahuja R and Schneider J M 2003 *Phys. Rev.* B **68** 224112
[5] Wang J Y and Zhou Y C 2004 *Phys. Rev.* B **69** 144108
[6] Kumar R S, Rekhi S, Cornelius A L and Barsoum M W 2005 *Appl. Phys. Lett.* **86** 111904
[7] Onodera A, Hirano H, Yuasa T, Gao N F and Miyamoto Y 1999 *Appl. Phys. Lett.* **74** 3782
[8] Manoun B, Gulve R P, Saxena S K, Gupta S, Barsoum M W and Zha C S 2006 *Phys. Rev.* B **73** 024110
[9] Segall M D, Lindan P L D, Probert M J, Pickard C J, Hasnip P J, Clark S J and Payne M C 2002 *J. Phys.: Condens. Matter* **14** 2717
[10] Vanderbilt D 1990 *Phys. Rev.* B **41** 7892
[11] Perdew J P, Cherary J A, Vosko S H, Jackson K A, Pederson M R, Singh D J and Fiolhais C 1992 *Phys. Rev.* B **46** 6671
[12] Monkhorst H J and Pack J D 1977 *Phys. Rev.* B **16** 1748
[13] Pfrommer B G, Côté M, Louie S G and Cohen M L 1997 *J. Comput. Phys.* **131** 233
[14] Blaha P, Schwarz K and Luitz J 1999 *Computer Code WIEN2k* Karlheinz Schwarz, Technical University Wien, Vienna
[15] Teter D M 1998 *MRS Bull.* **23** 22
[16] Jhi S H, Ihm J, Louie S G and Cohen M L 1999 *Nature* **399** 132
[17] Wang J Y, Zhou Y C, Lin Z J, Liao T and He L F 2006 *Phys. Rev.* B **73** 134107
[18] Liao T, Wang J Y and Zhou Y C 2006 *Phys. Rev.* B **73** 214109
[19] Jhi S H, Louie S G, Cohen M L and Morris J W 2001 *Phys. Rev. Lett.* **87** 075503
[20] Nye J F 1985 *Physical Properties of Crystals: Their Representation by Tensors and Matrices* (Oxford: Clarendon)
[21] Sun Z M, Music D, Ahuja R and Schneider J M 2005 *J. Phys.: Condens. Matter* **17** 7169